Biochimica et Biophysica Acta, 548 (1979) 348—373

BBA 47740

STRUCTURAL STUDIES ON RECONSTITUTED REACTION CENTER-PHOSPHATIDYLCHOLINE MEMBRANES

JAMES M. PACHENCE [a], P. LESLIE DUTTON [b] and J. KENT BLASIE [a]

[a] *Department of Chemistry and Biochemistry/Biophysics and* [b] *Department of Biochemistry and Biophysics, University of Pennsylvania, Philadelphia, PA 19104 (U.S.A.)*

(Received April 11th, 1979)

Key words: Reaction center; Cytochrome c; Electron transfer; Chromatophore; Membrane reconstitution; Phosphatidylcholine bilayer; (Rps. sphaeroides R26 mutant, X-ray diffraction)

Summary

Reaction center protein, isolated from the photosynthetic bacterium *Rhodopseudomonas sphaeroides* R26 mutant, was incorporated into phosphatidylcholine bilayers forming a homogeneous population of unilamellar vesicles. Cytochrome *c*, added to preformed reaction center-phosphatidylcholine vesicles, rapidly reduced up to 90% of the laser-generated $(BChl)_2^+$ of the reaction center (with kinetics of electron transfer similar to those in the chromatophore membrane) which suggests that the portion of the reaction center which accommodates functional cytochrome *c* binding sites is exposed predominantly on the exterior of the vesicles.

Unit cell electron density profiles were derived from lamellar X-ray diffraction from oriented reaction center-phosphatidylcholine membrane multilayers at varying lipid/protein ratios. The analysis of these profiles showed that the reaction center protein incorporates into the phosphatidylcholine membrane with unique sidedness and that the profile of the reaction center protein itself is asymmetric and spans the membrane.

Introduction

Light-harvesting pigments of photosynthetic membranes of plants and photosynthetic bacteria transfer captured light quanta to special (bacterio)-chlorophyll proteins called reaction center proteins. Reaction centers catalyze

Abbreviations: $(BChl)_2$ and $(BChl)_2^+$, the reaction center bacteriochlorophyll dimer in reduced and oxidized form, respectively; BPh, bacteriopheophytin; SDS, sodium dodecyl sulfate.

the conversion of the light energy into electrochemical free energy via a series of light-induced electron transfer reactions. Most of the pioneering work into mechanisms involved in the energy conversion has been done on reaction centers from the chromatophore membranes of photosynthetic bacteria, in particular from the blue-green mutant R26 or *Rhodopseudomonas sphaeroides*. The reaction centers from this organism have a molecular weight of about 70 000 [1] and contain the following components: four bacteriochlorophylls (BChl), two bacteriopheophytins (BPh), two ubiquinones (Q), and one iron atom (see Ref. 2). Two of the BChls occur in the form of a dimer $(BChl)_2$ which upon excitation undergoes oxidation in less than 10 ps to form $(BChl)_2^+$. One of the BPh goes reduced in this time to form BPh^-. Bph^- reduces one of the ubiquinones (which is weakly associated with the iron) to form the semiquinone (Q^-(Fe)) with a half-time of 100—200 ps [3,4]. The electron then continues via the second ubiquinone to reduce other components not directly associated with the reaction center. The $(BChl)_2^+$ is subsequently reduced by cytochrome c_2 located in the inner aqueous space of the chromatophore vesicle [5,6].

There is indirect evidence that the reaction center spans the chromatophore membrane (see Ref. 2) and that the cytochrome *c*-reaction center complex transfers electrons across the membrane (see Ref. 7). In order to investigate the resulting structural requirements placed on the reaction center protein in the membrane, we have undertaken to study the structure of isolated reaction center protein incorporated into a membranous environment.

Information on the structure and position of the reaction center in the reconstituted membrane can be obtained if the membranes can be organized in a crystalline or semi-crystalline state such as in hydrated oriented multilayers [8—11]. Analysis of unit cell electron density profiles derived at 10—15 Å resolution from the lamellar X-ray diffraction of reaction center-phosphatidylcholine membrane multilayers as a function of lipid/protein ratio has provided information concerning the reaction center protein structure and position with respect to the membrane profile. In addition, this study investigates the reconstituted phosphatidylcholine-reaction center membrane multilayers from a functional point of view showing that the protein retains accepted kinetic as well as optical absorption characteristics.

A preliminary study of cytochrome c_2 oxidation in a reconstituted system and X-ray diffraction studies on this system have been briefly reported elsewhere [12—14].

Materials and Methods

Reaction center preparation

Rps. sphaeroides R26 cells were grown in a mineral medium containing succinate as the sole carbon source, as previously described [5]. Reaction centers were prepared after the method of Clayton and Wang [15]. An index for purity was established from a combination of data from SDS gel electrophoresis (see Ref. 16) and absorption spectroscopy. An absorption scan at 280 nm of the gels for the reaction center preparation revealed only three bands at 20 000, 24 000, and 27 000 molecular weight associated with the reaction cen-

ter [1,16]. The ratios of absorbance at 280—800 nm ($A_{280/800}$) and 800—865 nm ($A_{800/865}$) were used to provide a spectral indication of protein purity. The first ratio compares the absorbance at 280 nm which includes general protein absorbance to the most intense reaction center chromophore absorbance at 800, which is assigned to the BChl of the reaction center; values for $A_{280/800}$ have been reported in the range of 1.22—1.5 for purified reaction center protein [1,15,17] while the lower and upper limits in our preparations have been 1.28—1.35. The values of $A_{800/865}$ (the 865 nm band represents $(BChl)_2$ absorbance) have been reported to be 2.2—2.5 for purified reaction center [1,15, 17]; the reaction center preparations used in this study had a ratio in the range of 2.1—2.3.

Preparation of lipids

Egg phosphatidylcholine was isolated from fresh egg yolks, according to the method developed by Singleton et al. [19]. The phosphatidylcholine was analyzed using thin-layer chromatography and gas chromatography [20].

Lipid-protein membrane preparation

Phosphatidylcholine-reaction center dispersions. The method used for the preparation of phosphatidylcholine-reaction center membrane dispersions utilized the ability to eliminate LDAO as a detergent by chemical reduction, the product being a tri-alkylamine: (i) reaction centers in lauryldimethylamine oxide were dialyzed in 10 mM Tris (pH 8) and 0.1% lauryldimethylamine oxide for 2 h to eliminate salts; (ii) the appropriate amount of egg phosphatidylcholine in solvent was dried under argon in a vessel equipped for sonication and anaerobic redox potentiometry [21]; (iii) the reaction center-lauryldimethylamine oxide suspension was added to the vessel. The vessel was kept at 20°C with minimal light under an atmosphere of argon; (iv) a fresh solution of sodium dithionite at pH 9 was added in microliter amounts while sonicating (Branson 'microtip', low power at 10 kHz) until the E_h was steady at about —250 mV (the reduction of lauryldimethylamine oxide occurs at significant rates below 0 mV), and (v) the reduced mixture was dialyzed with 10 mM Tris for 40 h to remove products of the reduction. Variation of this technique (i.e. temperature during sonication, E_h, time of dialysis, etc.) resulted in oriented membrane multilayers which possessed greater disorder and/or a lesser degree of orientation.

Phosphatidylcholine-reaction center/cytochrome c dispersions. Reduced cytochrome *c* (horse heart, obtained from Sigma, St. Louis, MO; type IV) was added to the dispersion of phosphatidylcholine-reaction center membranes in the experiments for measuring cytochrome *c* binding and kinetic activity with the reaction centers. The binding experiments were done by separating the phosphatidylcholine-reaction center membranes from the supernatant by ultracentrifugation (see next section). The phosphatidylcholine-reaction center/cytochrome *c* pellet, sedimented onto Mylar, was assayed spectrophotometrically to determine the ratio of bound cytochrome *c* to reaction center. The supernatant was also assayed for unbound cytochrome *c*; there was no measurable amount of reaction center or lipid in the supernatant in all experiments. Unless specifically stated in the text, reduced cytochrome *c* was added after the final step

of phosphatidylcholine-reaction center membrane formation. However, in our investigation of the nature of the cytochrome *c* association with the phosphatidylcholine-reaction center membranes, the cytochrome *c* was sometimes added together with the reaction center-lauryldimethylamine oxide suspension to the phosphatidylcholine, prior to the sonication.

Preparation of hydrated, oriented multilayers from phosphatidylcholine-reaction center dispersions

Aliquots of the phosphatidylcholine-reaction center dispersions (approximately 0.2—0.4 mg of protein for the X-ray experiments) were sedimented by ultracentrifugation (70 000 × *g* for 3 h) onto an aluminum foil strip using a demountable lucite sedimentation cell, as previously described [9]. The aluminum strip containing a 5 mm diameter fully hydrated membrane multilayer was attached to a 1 cm square glass slide which has a cylindrical curvature of 0.5 cm^{-1}. The multilayers were partially dehydrated for more than 20 h at 6°C over a saturated salt solution under argon or helium before exposure. The difference between the weight of the partially dehydrated and the fully dehydrated multilayer was taken to be the multilayer water content. Table I presents typical water contents of the multilayers investigated.

For absorption spectroscopy and flash-induced kinetic spectroscopy, multilayers (10 mm diameter) were formed on Mylar in an identical manner. The amount of protein was increased to insure that the multilayer thickness was consistent with the X-ray experiments.

Sedimentation of lipid-reaction center/cytochrome *c* dispersions was done in an analogous way. The cytochrome *c* content of the multilayer was checked by spectrophotometric assay of the reduced minus oxidized difference spectrum of the cytochrome *c*, both in the multilayer and the supernatant.

Kinetic studies

Fast oxidation-reduction reactions (microsecond resolution) were measured spectrophotometrically using a fast dual-wavelength instrument; absorption measurements for the redox changes of $(BChl)_2$ and cytochrome *c* were measured at 605 nm minus 540 nm and 550 nm minus 540 nm, respectively [5]. The reactions were activated using a 20 ns Q-switched ruby laser pulse. The laser pulse was intense enough to convert essentially all the $(BChl)_2$ into the $(BChl)_2^{\ddagger}$ form [22] and short enough to turn the system over once. The measuring beams were perpendicular to each other, and the direction of the laser

TABLE I

MULTILAYER WATER CONTENT

RH, relative humidity.

Lipid/protein	Water content (%)	
	RH = 95%	RH = 90%
150/1	40 ± 2	38 ± 2
100/1	37 ± 2	34 ± 2
75/1	37 ± 2	33 ± 2

pulse was perpendicular to the plane of the measuring beams.

When kinetics were measured in the multilayers, the Mylar supports were placed so that the perpendicular to the Mylar plane made a 45° angle with respect to each measuring beam. The perpendicular to the Mylar plane made about a 10° angle with the plane of the measuring beams.

X-ray diffraction equipment

The lamellar X-ray diffraction from the membrane multilayers was recorded on Ilford type G X-ray film utilizing the X-ray equipment described in detail in Ref. 9.

X-ray data reduction

The lamellar X-ray diffraction data on film were converted to digital form as a function of s ($s = 2\sin\theta/\lambda$, where s is the reciprocal space coordinate, 2θ is the laboratory scattering angle, and λ is the X-ray wavelength) using a Joyce-Loebl' MK-IIICS microdensitometer. The shape of the background scattering from the membrane multilayers was estimated from the shape of non-Bragg lamellar scattering from highly ordered phosphatidylcholine multilayers. The phosphatidylcholine-reaction center membrane multilayeres produce a series of sharp lamellar reflections and the intensity between the reflections generally approached the estimated background scattering. In these cases, the estimated background scattering can be subtracted from the total lamellar diffraction data after the background scattering was scaled to both the high and low-angle regions of the data. Similar background subtraction procedure have led to reasonable results in other systems [9]. After eliminating the background scattering, the lamellar diffraction must be corrected by a factor of s^2. One fractor of s is due to the intersection of the reciprocal lattice for these cylindrically curved multilayers with the Ewald sphere (Lorentz correction factor). Another factor of s is required since the patterns exhibited measurable mosaic spread and the resulting arced lamellar diffraction on the film was measured with a fixed slit height that was small with respect to the length of the arcs. This corrected lamellar diffraction data from swelling experiments [23] was analyzed using a PDP-10 computer according to the algorithm developed by Stamatoff and Krimm [24].

Results

Properties of reaction centers incorporated into egg phosphatidylcholine and the interaction with cytochrome c

Fig. 1 reveals that the reaction centers incorporated into egg phosphatidylcholine produce an absorption spectra similar to reaction centers solubilized in lauryldimethylamine oxide. However, closer investigation reveals that the ratio of $A_{800/865}$, and absorbance at 595 nm is diminished for phosphatidylcholine-reaction center dispersions (not shown) and the multilayers, as compared to reaction center-lauryldimethylamine oxide suspension. The origins of this change are under investigation but preliminary work indicates that the change is not a result of protein denaturation or chromophore loss since the above effects are reversed when the reaction center is returned to an lauryldimethylamine oxide environment.

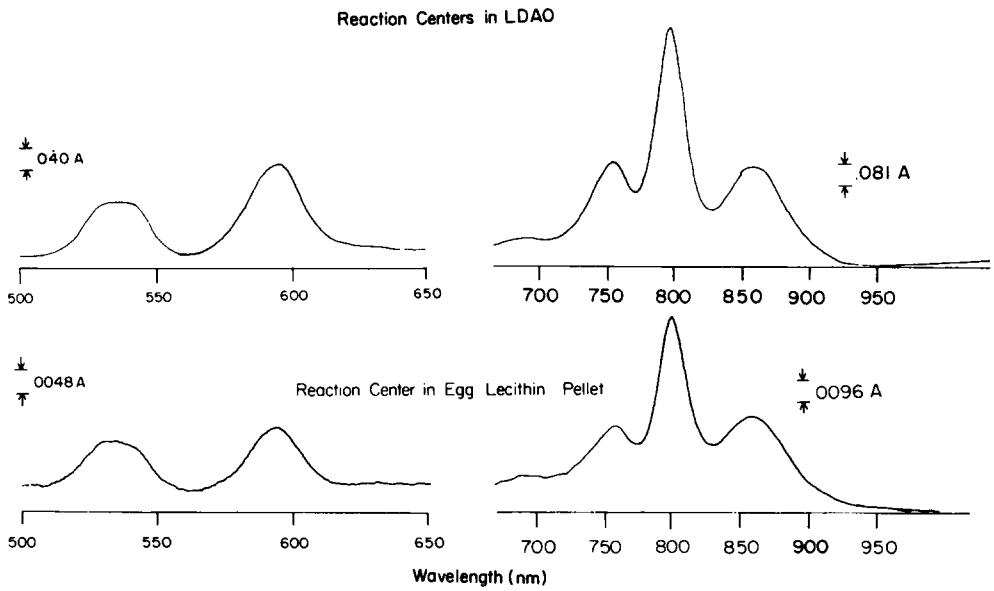

Fig. 1. Absorption spectra of reaction centers. The upper traces were measured on reaction center protein in 0.1% lauryldimethylamine oxide, and the lower traces on oriented membrane multilayers of reaction centers incorporated into egg phosphatidylcholine, with lipid/protein = 100, relative humidity of 90%. The spectra were run at room temperature.

We have used mammalian cytochrome *c* added to preformed phosphatidylcholine-reaction center dispersions to test the accessibility of the $(BChl)_2$ of the reaction center to the external aqueous phase. Fig. 2 shows the reduction of flash-induced $(BChl)_2^+$ with no cytochrome *c*, a cytochrome *c*/reaction center ratio of 2, and a cytochrome *c*/reaction center ratio of 20. As expected, there is very little re-duction of the flash-generated $(BChl)_2^+$ within the experimental

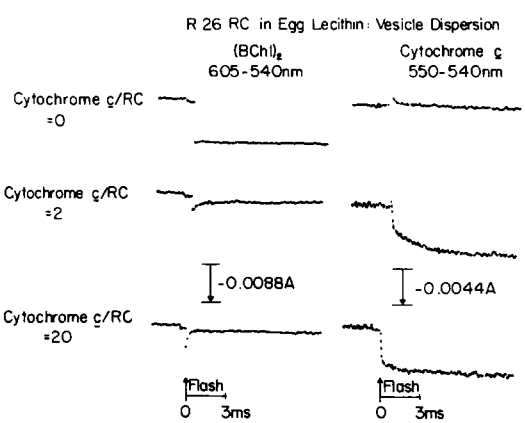

Fig. 2. Laser-activated kinetics of reaction center $(BChl)_2$ and cytochrome *c* oxidation-reduction at 12.8 ms full scale for phosphatidylcholine-reaction center vesicular dispersions (lipid/protein = 150) in 10 mM Tris, pH 8, at room temperature. The ratio of $(BChl)_2$ that was reduced by cytochrome *c* at 12.8 ms versus the full oxidation signal of $(BChl)_2$ in the absence of cytochrome *c* is a measure of the extent of the rapid re-reduction of $(BChl)_2$ by cytochrome *c*; it is also an indication of the availability of cytochrome *c* to $(BChl)_2$.

time of 12.8 ms when cytochrome *c* is not present. However, in the presence of ferrocytochrome *c*, much of the $(BChl)_2^+$ becomes promptly re-reduced well within the 12.8 ms experimental trace. Fig. 2 indicates that cytochrome *c* undergoes oxidation roughly concomitant with $(BChl)_2^+$ re-reduction. The kinetic traces of Fig. 2 are similar to those obtained previously in phosphatidylcholine-reaction center dispersions, but with cytochrome c_2 (Dutton, P.L., Petty, K.M., Bashford, C.L. and Prince, R.C., unpublished results).

It is important to note that the amount of $(BChl)_2^+$ available for prompt re-reduction by externally added cytochrome *c* approached 80% with the physiological ratio of two cytochrome *c*/reaction center; this value was further increased another 10% when the cytochrome *c* to reaction center ratio was 20/1 (Fig. 2).

These experiments were extended to examine cytochrome *c*-reaction center reactions in multilayers prepared by sedimenting dispersions of the phosphatidylcholine-reaction center membranes with externally added cytochrome *c* (see Materials and Methods). Starting with a cytochrome *c*/reaction center ratio of 2 under conditions similar to those of Fig. 2 it was evident after sedimentation that the supernatant contained no measurable levels of reaction center and approximately 10% of the initially added cytochrome *c*, implying that the cytochrome *c* was firmly bound to the reaction center-containing membranes. This was confirmed by direct analysis of the cytochrome *c* and reaction center in the multilayer which showed the ratio to slightly less than 2. However, when an attempt was made to form a multilayer containing higher amount of cytochrome *c*/reaction center (e.g. starting with a cytochrome *c* to reaction center ratio of 20) a large quantity of cytochrome remained in the supernatant after centrifugation although the cytochrome *c* to reaction center ratio in the multilayer was increased to approx. 4:1. This ratio was reproducible from preparation to preparation with values always falling between 3:1 and 4:1. The kinetics of the flash-activated cytochrome *c* oxidation in multilayers (Fig. 2) appears to be similar to that encountered in the dispersion shown in Fig. 2. The extent of the $(BChl)_2^+$ re-reduced by cytochrome *c* in the multilayer was measured to be 78 and 89% for the cytochrome *c* to reaction center ratios of 2:1 and 4:1, respectively.

Nature of the phosphatidylcholine-reaction center dispersions

The phosphatidylcholine-reaction center dispersions that we used were optically clear, from which it may be deduced that the membranous particles must have dimensions that are small relative to the wavelength of visible light. Such dispersions (phosphatidylcholine-reaction center mol ratio of 100 or 50) were placed on a sucrose gradient composed of 1% steps between 20% and 40% sucrose and centrifuged at $10^5 \times g$ for 4—10 h. The particles were found in a single band at the interface between 32% and 33% sucrose indicating that such dispersions are relatively homogeneous in density.

If cytochrome *c* was present during the preparation of the phosphatidylcholine-reaction center dispersions, then it was apparent that cytochrome *c* was trapped within the particles; this was shown in Table II for dispersions prepared in media of low ionic strengths (with cytochrome *c* binding) and high ionic strengths (no cytochrome *c* binding). At low ionic strengths with cyto-

TABLE II

The initial buffer conditions were present during vesicle formation, and in the process of measuring the initial cytochrome *c* incorporation.

RC, reaction center.

Dispersion	Initial buffer conditions	Initial cytochrome *c*/(100 EL) ratio	Total initial cytochrome *c*/(100 EL) associated with the particles	Cytochrome *c*/(100 EL) remaining after the particles were washed with 1.0 M KCl
A. RC-phosphatidylcholine (lipid/protein = 100), cytochrome *c* added after particle formation	10 mM Tris-HCl, pH 8	1.00	0.75	0.0
		3.00	2.23	0.0
		6.00	3.40	0.0
B. RC-phosphatidylcholine, cytochrome *c* added during particle formation *	10 mM Tris-HCl, pH 8	1.00	0.95	0.25
		3.00	2.78	0.84
		6.00	4.48	1.38
C. RC-phosphatidylcholine, cytochrome *c* added during particle formation **	10 mM Tris-HCl, 1.0 M KCl, pH 8	1.00	0.50	0.45
		3.00	1.33	1.30
		6.00	2.50	2.46
D. Phosphatidylcholine, cytochrome *c* added during particle formation **	10 mM Tris-HCl, 1.0 M KCl, pH 8	1.00	0.58	0.55
		3.00	1.38	1.32
		6.00	2.80	2.78

* A significant amount of cytochrome *c* will bind to the reaction center with a buffer of just 10 mM Tris (A); hence, there is a difference between the amount of cytochrome c retained by the particles after 1.0 M KCl washes in this experiment versus that of experiment C, at the same initial cytochrome *c*/(100 EL) ratio.

** Negligible cytochrome *c* binding resulted when cytochrome *c* was added externally to pure EL or EL/reaction center vesicles in 10 mM Tris, 1.0 M KCl buffer. Therefore, experiments C and D represent the amount of cytochrome *c* trapped within EL/reaction center or pure EL vesicles, respectively.

chrome *c* present during the preparation of the dispersion, the amount of cytochrome *c* tightly associated with the particles was greater than the amount bound when cytochrome *c* was added externally (compare Table II, A and B); in concert with the idea that some cytochrome *c* was trapped inside the particle, these particles retained the extra cytochrome *c* after washing with 1.0 M KCl. There was no measurable binding of externally added cytochrome *c* in the present of 1.0 M KCl (Table IIA). Alternatively, with cytochrome *c* present during preparation at high ionic strengths, a similar amount of cytochrome *c* was trapped by the particles (Table IIC); soaking of the particles in 1.0 M KCl for 48 h failed to release cytochrome *c*. Furthermore, similar experiments (Table IID) using a sonicated dispersion of pure phosphatidylcholine alone (no reaction center) revealed that the amount of cytochrome *c* trapped within the egg phosphatidylcholine vesicles in 10 mM Tris, 1.0 M KCl was similar to the amount trapped by phosphatidylcholine-reaction center dispersions. Hence, these cytochrome *c* binding and trapping experiments indicate that the phosphatidylcholine-reaction center dispersions were vesicular since other particle structures which could possibly result from our reconstitution procedure would not be expected to trap and retain cytochrome *c*.

As seen in Fig. 2, over 85% of the photooxidized $(BChl)_2$ in these lipid-pro-

tein dispersions was available to cytochrome *c* added after preparation of the dispersions. This result would be expected only if the lipid-reaction center dispersions consisted of unilamellar, as opposed to multilamellar, vesicles. Hence, these lipid-protein dispersions apparently consist of a homogeneous (in density) population of unilamellar membraneous vesicles which can be visualized in electron micrographs of negatively stained dispersions (not shown). We can also conclude that the reaction center protein must be distributed asymmetrically within the membrane profile of these unilamellar vesicles to account for the accessibility to cytochrome *c* bound only at the extravesicular surface.

Characteristics of the X-ray diffraction patterns

A series of X-ray diffraction experiments were performed on the reconstituted membrane multilayers utilizing what we have found to be optimal conditions. These conditions, which included slow partial dehydration of the multilayers at 90—95% relative humidity at 6°C under argon, provided lamellar diffraction which exhibited minimal degrees of lattice disorder and mosaic spread and most intense higher-angle diffraction extending to $s \approx 1/9$ Å. Changing relative humidity after the initial partial dehydration did not significantly alter the quality of the diffraction (see Fig. 5).

Lamellar diffraction was recorded from multilayers of pure phosphatidylcholine (Fig. 4) and from multilayers of different lipid to reaction center pro-

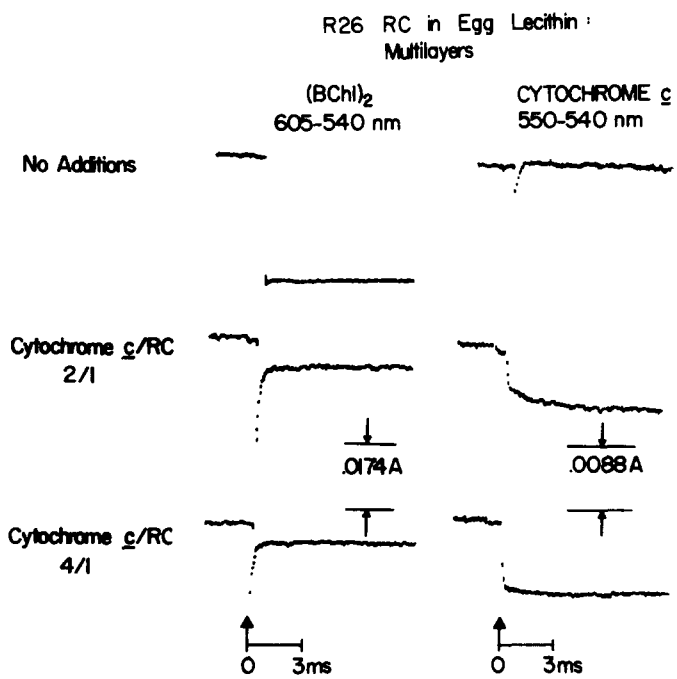

Fig. 3. Laser-activated kinetics of reaction center $(BChl)_2$ and cytochrome *c* oxidation-reduction on phosphatidylcholine-reaction center multilayers, with a time scale of 12.8 ms. Dispersions of phosphatidylcholine-reaction center vesicles (lipid/protein = 150) in 10 mM Tris-HCl, pH 8.0, were centrifuged in the presence of varying amounts of cytochrome *c* (added after formation of the phosphatidylcholine/reaction center vesicles). The ratio presented was the amount of cytochrome *c* retained by the phosphatidylcholine-reaction center membranes.

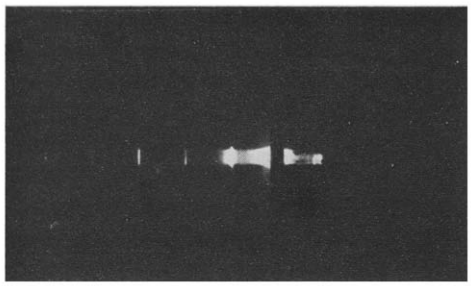

Fig. 4. Lamellar X-ray diffraction from pure phosphatidylcholine multilayers, with relative humidity of 81% at 6°C.

tein molar ratios of 150/1, 100/1, 75/1 and 50/1 (Figs. 5 and 6). The lamellar diffraction, recorded on film, was microdensitometered (Fig. 7), coverted to digital form and then corrected as discussed in Materials and Methods (Table V). Overlap from neighboring diffraction orders was negligible even at higher diffraction angles for all lipid/protein ratios investigated. This characteristic helped determine the actual background scattering in regions of the lamellar diffraction where the background scattering level was above the estimated level due to incoherent (diffuse) lamellar scattering from the multilayer (the portion of Fig. 7 from $6/D$ to $10/D$ exhibits background scattering that is greater than that estimated in Materials and Methods).

Investigation of the X-ray patterns in Figs. 5 and 6 indicates that the mosaic spread remains nearly the same for the lipid to protein ratios investigated (less than 6°). The information in Table III indicates that all the phosphatidylcholine-reaction center multilayers retain some residual lattice disorder. As also can be determined from Table III, overlap of neighboring orders does exist to a small extent only at higher diffraction angles (orders 5—8) for a lipid to

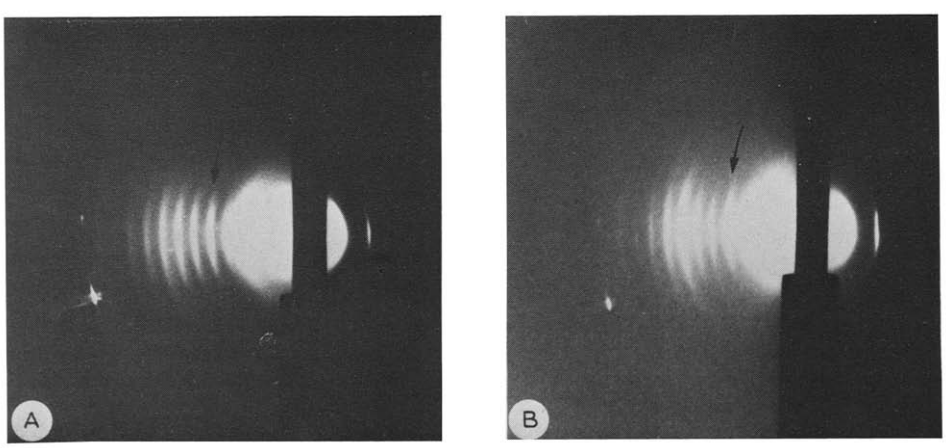

Fig. 5. Lamellar X-ray diffraction patterns from multilayers comprised of reaction centers and freshly isolated phosphatidylcholine, lipid/protein = 100, 6°C at (A) relative humidity = 90%, and (B) relative humidity = 95%. The quality of the diffraction pattern does not change when the water content is altered slightly. Arrows denote the position of the fifth-order reflection.

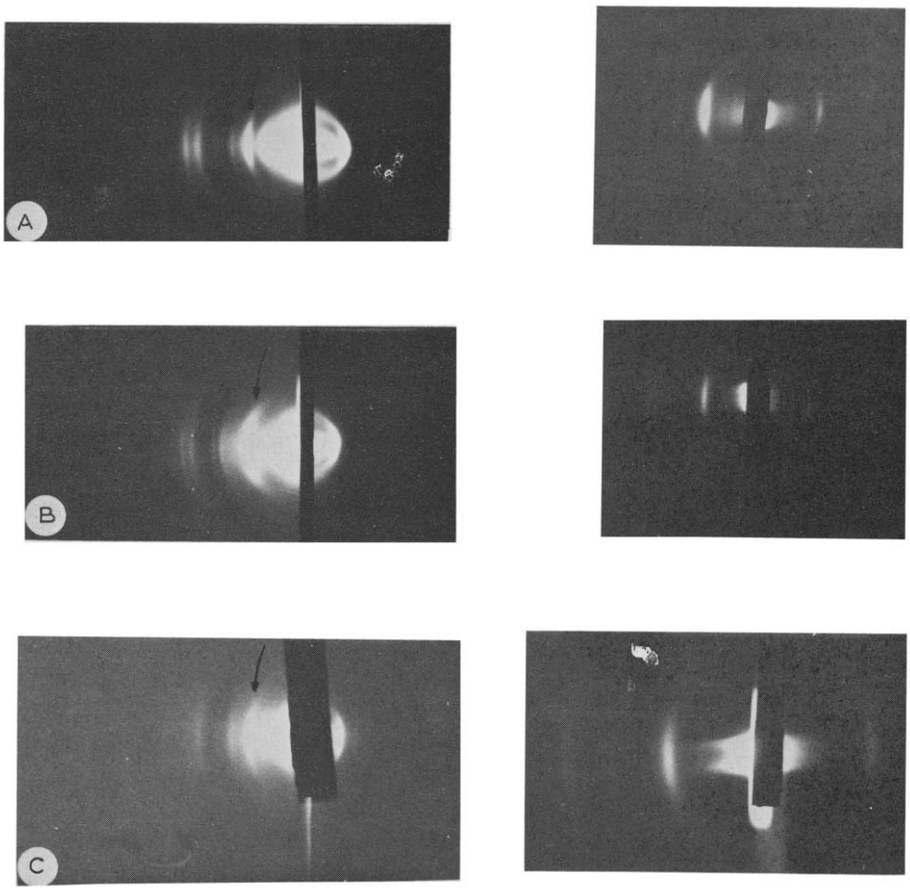

Fig. 6. Lamellar X-ray diffraction patterns from multilayers comprised of reaction centers and freshly isolated phosphatidylcholine, relative humidity of 90% at 6°C; (A) lipid/protein = 150; (B) lipid/protein = 75, and (C) lipid/protein = 50. The specimen to film distance for the patterns on the left was 62.5 mm, exposed for approximately 16 h and those on the right were at 250 mm, exposed for approximately 4 h, to view the lower orders. Arrows denote the position of the fourth-order reflection.

protein ratio of 50/1. Indeed, only at this lipid to protein ratio does lattice disorder become significant for this system. The highest-angle lamellar diffraction obtained for the phosphatidylcholine-reaction center multilayers extended to $s \approx 1/9$ Å for the 100/1 lipid-to-protein samples, while the bulk of the data extended to $s \approx 1/14$ Å.

Low-angle equatorial diffraction was not observed under our experimental conditions for any of these multilayer systems, except for the impure reaction center-commercial egg phosphatidylcholine multilayers of a preliminary study [13]. In principle, equatorial diffraction should be seen in all cases; however, the equatorial diffraction is considerably less intense than the lamellar diffraction and our experimental conditions were not optimized for recording such equatorial diffraction.

Nature of the oriented membrane multilayers

We note that the lamellar reflections from pure egg phosphatidylcholine-

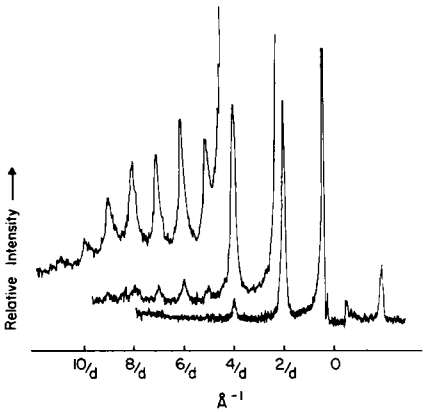

Fig. 7. Microdensitometer trace from the lamellar X-ray diffraction pattern of Fig. 5A, showing three separate scales to clearly show the higher-order lamellar reflections. D = 128 Å.

oriented multilayers (Fig. 4) occurred at $s = h/D$ for h = 1—6, where D was 50—60 Å (depending on the water content). The periodicity of multilayers consisting of phosphatidylcholine-reaction center membranes (D') was substantially different than D of the pure phosphatidylcholine multilayers (D' was approximately 125—130 Å, depending on water content) even for phosphatidylcholine-reaction center membranes having a large lipid-protein ratio. However, the water content for the phosphatidylcholine-reaction center membrane multilayers was approximately equal to or lower than that for the pure phosphatidylcholine multilayers. Table IV shows that the even order lamellar reflections at h = 2, 4 were generally strong compared to the odd orders at h = 1, 3, 5 from the phosphatidylcholine-reaction center multilayers at the various lipid/protein ratios; this information, together with the large multilayer periodicities ($D' \approx 2D$) and lower water contents as compared with pure phosphatidylcholine multilayers, strongly suggests that the unit cell for the phosphatidylcholine-reaction center multilayers contains two single membrane profiles. Lamellar neutron diffraction from these phosphatidylcholine-reaction center multi-

TABLE III

WIDTH AT HALF-MAXIMUM AS A FRACTION OF 1/D

Order Periodicity (D) Lipid/protein	125 Å 150 : 1	128 Å 100 : 1	128 Å 75 : 1	128 Å 50 : 1
1			0.227	0.227
2	0.187	0.200	0.195	0.227
3	0.218			0.390
4	0.250	0.200	0.227	0.358
5	0.250	0.266	0.227	0.358
6	0.343	0.266	0.227	0.520
7	0.286	0.266	0.266	
8	0.286	0.333	0.390	0.520
9	0.406	0.333		

TABLE IV

Δ VALUES

Lipid/protein	First phase choice	Second phase choice
150/1	0.0380	0.0411
100/1	0.0135	0.0201
75/1	0.0092	0.0120
50/1	0.1186	0.1305

layers supports this conclusion in that it clearly demonstrates the existence of three water layers and two lipid hydrocarbon layers within the unit cell profile (the lamellar neutron diffraction from these multilayers in 100% ^2H_2O exhibits a strong reflection as $s = 2/D'$ and much weaker reflections at $s = 1, 3, 4/D'$). Conversely, stacks of membrane sheets and stacks of flattened multilamellar ('onion skin') vesicles for these membrane systems would only be expected to produce discrete reflections at $s = h/D''$, where D'' is only slightly greater than the thickness of a single membrane profile, i.e. $D'' \simeq D \simeq D'/2$.

Hence, inspection of the lamellar X-ray and neutron diffraction from these phosphatidylcholine-reaction center multilayers clearly indicates the presence of two membrane profiles within the unit cell profile. This result is consistent with the assumption that these membrane multilayers were composed of stacks of flattened unilamellar membrane vesicles; stacks of membrane sheets or flattened multilamellar membrane vesicles occurring within the multilayers is not consistent with the lamellar diffraction results since their apparent unit cell profile contains only a single membrane profile.

X-ray diffraction analysis

As discussed in the previous section, the oriented multilayers contain stacks of flattened lipid-protein vesicles; the average orientation of the stacking axes in the multilayer is normal to the multilayer support. Neglecting edge effects, one flattened vesicle produces two membranes in the multilayer unit cell which clearly have a mirror plane of symmetry in the profile projection between them [27]. This situation produces a center of symmetry for the unit cell profile $\rho o(z)$, and therefore the corresponding phase factors for the lamellar reflections are limited to +1 or −1. Hence, there exist in general for such systems $2^{h_{max}}$ possible phase combinations for h_{max} lamellar reflections [24]; however, in a diffraction experiment $\rho o(z)$ cannot be distinguished from $-\rho o(z)$ and therefore only $2^{h_{max}-1}$ possible phase combinations need to be investigated, the first-order lamellar reflection phase being arbitrary.

Certain criteria must be satisfied before applying phasing methods utilizing data from swelling experiments. The lamellar diffraction maxima should remain relatively sharp so that the overlap between neighboring reflections is negligible. Any lattice-disorder effects can then be ignored when calculating an electron density profile provided that the integrated value of the lamellar reflection is used in the diffraction analysis (defined as $I'(h/D)$. It also is important that the mosaic spread and lattice disorder for a multilayer not change appreciably when the water content is varied in order to minimize errors in the inte-

gration of lamellar reflections. However, the water content does not have to change by more than a few percent (see Table I); under this condition, the only significant change is in the sampling interval of the lattice interference function, without significant changes in the unit cell profile.

The swelling experiment yields sets of lamellar diffraction data from the same multilayer sample, any pair of which produce two unit cell electron density profiles that are related by:

$$\rho_1(z) = A\rho_2(z) + B \tag{1}$$

where A is a scale factor, and B is related to $I_1(0)$ and $I_2(0)$, the lamellar origin reflections. An algorithm developed by Stamatoff and Krimm [24] can be used to phase the lamellar diffraction data from swelling experiments using the integrated lamellar reflection data directly. The method produces a value Δ for each phase combination which is a measure of least-squares difference between the right and left sides of Eqn. 1 integrated over the unit cell. The Δ values are sorted, with the smallest Δ corresponding to the most probable phase combination.

The ambiguity of sign for $\pm\rho o$ can usually be resolved by simple methods. First, the measured water content of the multilayer can restrict the regions identified with aqueous spaces in the unit cell profile. Second, the unit cell should swell within this aqueous region. Third, the choice must be consistent with the electron density characteristics of the membrane components; for instance, all profiles in this study exhibit regions of high electron density at the surfaces of the reconstituted membranes, features usually associated with the phospholipid head groups in a phospholipid bilayer profile which would be expected especially for the larger lipid/protein ratios. Also, experiments to directly investigate the distribution of water in the unit cell profiles (i.e. neutron diffraction) must be consistent with the X-ray diffraction results.

Calculated unit cell electron density profiles

The unit cell electron density profiles calculated as previously described, contain two asymmetric membranes, with a range of membrane thickness from 58 Å to 62 Å and unit cell dimensions of 126—138 Å (depending on the lipid to protein ratio). The profiles in Fig. 9 generally resemble two lipid bilayers. The asymmetry is generally confined to the surfaces of the membranes although significant changes also occur near the center of the membranes. The most probable phase choice for the various lipid/protein ratios is statistically significant as can be determined from Table IV, the experimental errors in integrated lamellar reflections (Fig. 7) and the complete error analysis presented with the algorithm by Stamatoff and Krimm [24].

To aid in the analysis of the structural profiles of the reaction center-phosphatidylcholine reconstituted membranes, the unit cell electron density profiles of Figs. 8 and 9 were converted to their step-function equivalents (Fig. 10). It was convenient to compare the various profiles in this way as the true amplitudes and widths of the various features in the profiles of Fig. 9 are obscured by truncation errors in the Fourier syntheses. Therefore, the progressive changes from increasing protein content can be readily observed in these step-function profiles (Fig. 10).

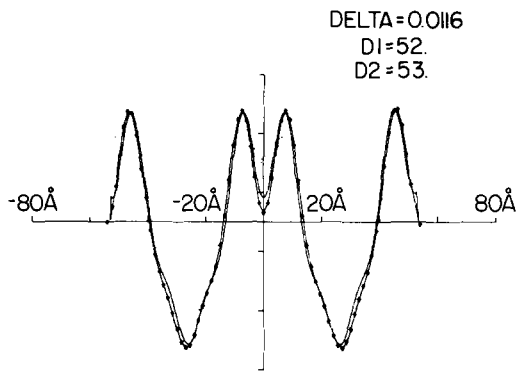

Fig. 8. Electron density profile of egg phosphatidylcholine, calculated from the pattern of Fig. 4, and another done at a relative humidity of 90%. The unit cell consists of one symmetric membrane, centered at 26 Å. Two unit cells are shown for comparison with Fig. 9.

The step-function amplitudes of the unit cell profiles were estimated directly from the corresponding amplitudes in Fig. 9. The uncertainty in these amplitudes is determined solely by the experimental accuracy of the integrated reflection data, and consequently by the correct phase choice. The widths of the step functions were initially taken to correspond to the most prominent features of the experimental electron density profile, having dimensions on the order of $D/h_{\max}$ (thereby generating step-function equivalent profiles composed of approximately $h_{\max}$ steps). This initial step-function profile was used to calculate integrated lamellar reflection data ($I_C(h/D)$) and subsequently, a re-calculated unit cell profile ($\rho c(z)$) via successive Fourier transformations. A least-squares R value was determined for the calculated versus the derived unit cell electron density profile:

$$R_\rho = \sum_{z=-D/2}^{D/2} [\rho o(z) - \rho c(z)]^2 / \sum_{z=-D/2}^{D/2} [\rho o(z)]^2 \qquad (2)$$

The step-function profiles were first refined in real space by varying the widths (over a relatively narrow range of ±2 Å, as determined by the derived profiles $\rho o(z)$ in Fig. 9) and amplitudes (also over a relatively narrow range defined by $\rho o(z)$) of the step functions in accordance with a strict comparison of $\rho o(z)$ and $\rho c(z)$ until a minimum R_ρ value was obtained. It should be noted that since both the amplitudes and the phases of the lamellar reflections have been determined for $h_{\max}$ reflections, the number of variables permitted in this refinement is less than $2\,h_{\max}$. Since the amplitudes were not freely varied (as described), we have in fact utilized on the order of $h_{\max}$ free variables, which is considerably less than $2\,h_{\max}$. The step-function profiles from the preceding calculations were used for placing the profiles on an absolute electron density scale and, as will be detailed in the next section, when attempting to calculate the protein structure profile; the protein structure profile can be obtained if the proper lipid profile is subtracted from the phosphatidylcholine/reaction center membrane profile.

Further refinement was done on the step-function profile to produce a more

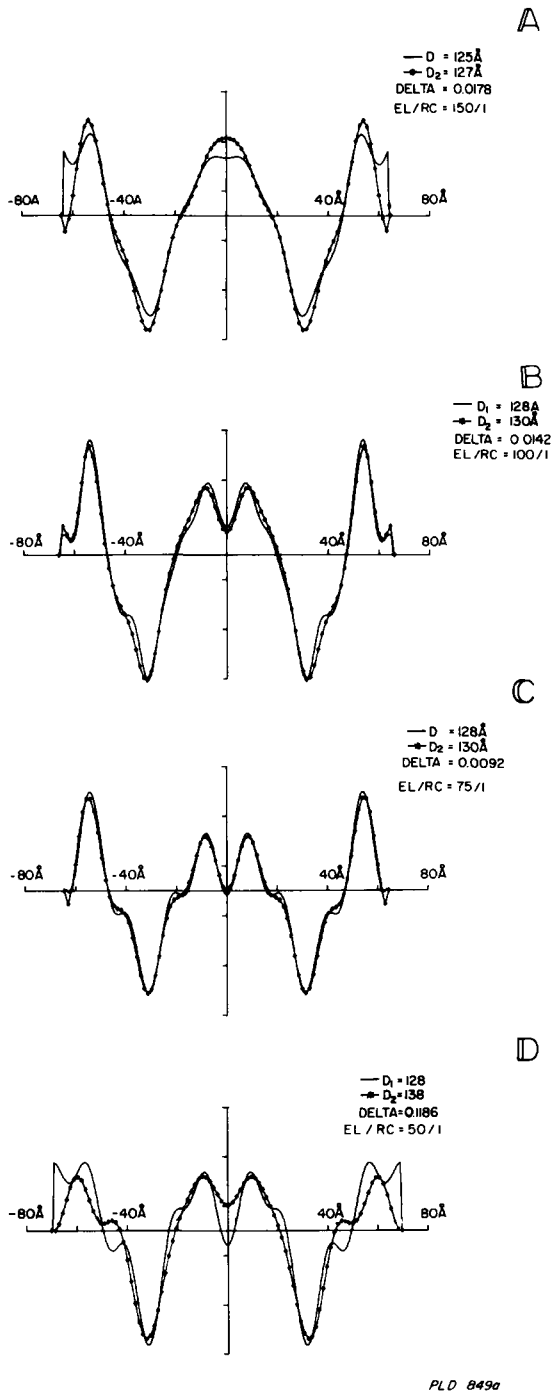

Fig. 9. Electron density profiles, calculated from lamellar X-ray diffraction patterns from oriented multilayers of phosphatidylcholine/reaction center (see Figs. 5 and 6). One unit cell is shown for each profile, comprised of two membranes/unit cell. The lamellar X-ray diffraction was phased by a multilayer swelling technique. Unit cells of the same multilayer at relative humidities of 90% and 95% are superimposed, showing that only slight changes occur upon swelling.

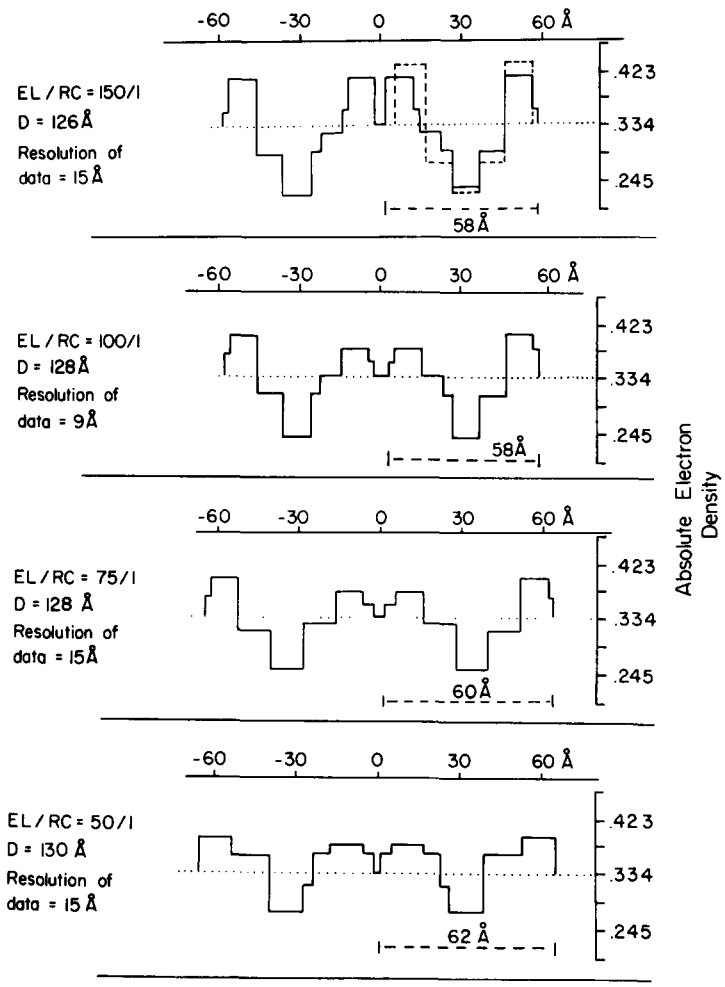

Fig. 10. Step-function profiles were calculated directly from the unit cell electron density profiles of the phosphatidylcholine/reaction center membranes and put on an absolute scale to aid in the structural analysis. The electron scale is at the right of each figure, where the dotted line through the center of the scale denotes the electron density level of water. The progressive changes in the membrane profiles upon increasing protein content (phosphatidylcholine/reaction center ratios range from 150 to 50) can be readily observed. The step-function profile for phosphatidylcholine, calculated directly from Fig. 8, is superimposed on the top figure (- - - - -). The extent of each membrane is noted on the bottom right of each figure. The protein structure profile can be obtained from the step-function profiles by subtracting the proper phosphatidylcholine profile from the phosphatidylcholine/reaction center membrane profiles.

detailed $\rho c(z)$. The total number of steps were chosen to be the minimum number required to produce a $\rho c(z)$ with a R_ρ less than the experimental error (about 0.06). The amplitudes and widths of these additional steps (less than 6/profile) were again severely restricted by the derived profiles $\rho o(z)$ in Fig. 9, and therefore the number of free variables in this refinement was still less than $2\,h_{max}$.

In general, the absolute electron density at an arbitrary position in the unit

cell profile can be expressed as a function of the membrane constitutents:

$$\rho o(z) = \rho^{P}(z)f_{P} + \rho^{L}(z)f_{L} + \rho^{M}(z)f_{M} \quad (3)$$

which is simply the density of each component (P = protein, L = lipid, M = medium) multipled by the mol fraction f of the component. The assumption can be made that the electron density near the center of the phosphatidylcholine-reaction center membrane is composed almost exclusively of lipid hydrocarbon chains and protein; therefore, $\rho^{M}(z)\ f_{M}$ can be eliminated from Eqn. 2 when considering the region of $17 < |z| < 48$ Å within the unit cells in Fig. 9. The absolute electron density within one step of the step-function equivalent profiles (designated ρ_i, where the index i indicates a particular step) was calculated using Eqn. 3 to generate three equations for three different steps i, j and k near the center of the membrane:

$$\begin{aligned} \rho_i &= \rho_i^{P} f_{P} + \rho_i^{L} f_{L} \\ \rho_j &= \rho_j^{P} f_{P} + \rho_j^{L} f_{L} \\ \rho_k &= \rho_k^{P} f_{P} + \rho_k^{L} f_{L} \end{aligned} \quad (4)$$

Eqn. 4 is valid in the three step regions defined by $17\ \text{Å} < |z| < 28\ \text{Å}$, $28\ \text{Å} < |z| < 38\ \text{Å}$, and $38\ \text{Å} < |z| < 48\ \text{Å}$, as can be seen in Fig. 10. The composition of the membranes was known, hence the mol fractions f were known. The phosphatidylcholine electron density values ρ_i^{L}, ρ_j^{L} and ρ_K^{L} were calculated for the egg phosphatidylcholine bilayer profile, assuming an area of 70 Å^2/molecule [31]. The unknown quantities of Eqn. set 4 were reduced to three by noting that ρ_i, ρ_j and ρ_k are mutually proportional and likewise that ρ_i^{P} is proportional to ρ_k^{P}, assuming that the lipid bilayer is symmetric. These proportionality constants were obtained directly from Fig. 10. Therefore, solving Eqn. set 4 gave three points (ρ_i, ρ_j and ρ_k) on the absolute electron density scale, which is sufficient to scale the entire profile. The above scaling procedure indicated that the density of the step regions between membranes in the unit cell profiles were consistently $0.334 \pm 0.002\ e/\text{Å}^3$, which is in good agreement with the accepted value for an aqueous medium [28]. Preliminary neutron diffraction results have verified that these regions correspond to the aqueous medium (work in progress).

The preceding calculation implicitly assumes that (a) the mol fraction of the lipid component does not change from region to region in the membrane profile, and that (b) the electron density profile of egg phosphatidylcholine in the protein-lipid-reconstituted membranes is similar to the pure phosphatidylcholine profile. For instance, it is conceivable that more lipid may be displaced by protein on one side of the reconstituted membrane than the other; also, since the multilayers are formed from vesicles, curvature constraints may also produce a difference in the molar fraction of lipid components from one side of the membrane to the other. In the analysis that follows, it is indeed shown that the lipid electron density profile contribution to the reconstituted phosphatidylcholine-reaction center membrane cannot simply be the symmetric electron density profile of the pure lipid membrane (compare Figs. 11A and 13A). However, we note that the asymmetry in the lipid profile which we derived in the following section (Fig. 13A) does not significantly affect the

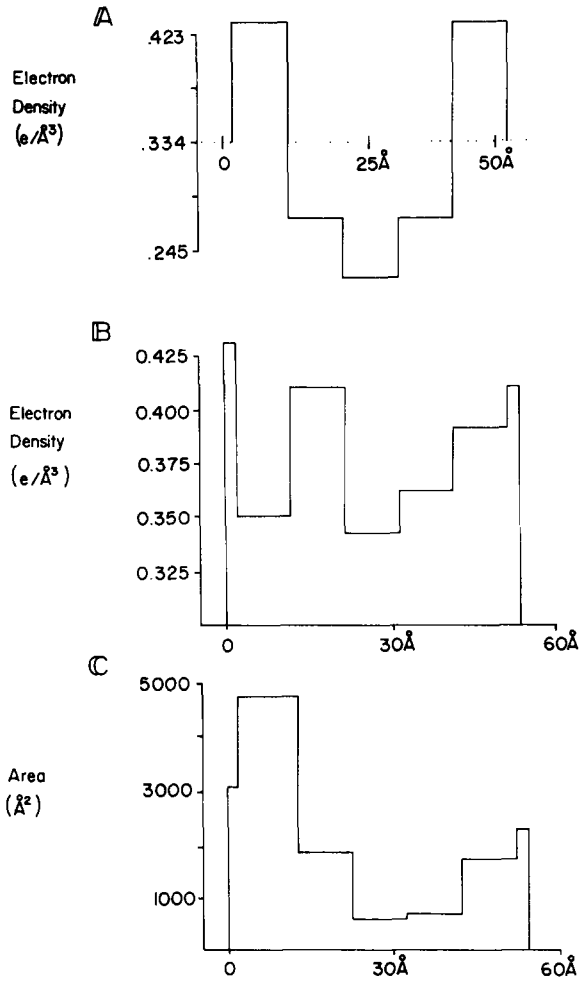

Fig. 11. (A) First approximation of the model lipid profile, calculated directly from the derived egg phosphatidylcholine profile; (B) Derived protein profile, shown as electron density versus position along the membrane profile-stacking axis. This calculation assumes a protein of constant area (0 Å refers to the center of the unit cell in Fig. 10). The calculation was done by subtracting the scaled lipid profile above from the membrane profile of Fig. 10A, lipid/protein = 150. (C) Area profile for the protein calculated in a fashion similar to that of (B) but assuming that the protein has constant electron density throughout the profile.

scaling of the profiles in Fig. 10.

Fig. 10A presents the step-function equivalent profile of pure lipid arbitrarily superimposed on the profile representing the highest lipid/protein ratio investigated. The most prominent perturbation of the lipid bilayer produced by incorporation of reaction center protein occurs at the edges of the reconstituted membranes, which are generally broader and less electron dense than the equivalent regions of the pure lipid bilayer. The center of the membrane increases in electron density as the protein component is increased relative to the lipid component.

TABLE V

CORRECTED INTENSITY AND CORRESPONDING PHASES

Order	Lipid/protein							
	150 : 1		100 : 1		75 : 1		50 : 1	
	ϕ	I'	ϕ	I'	ϕ	I'	ϕ	I'
1		0.0		0.0	−1	0.0279		0.0
2	+1	1.0	+1	1.0	+1	1.0	+1	1.0
3	−1	0.0453		0.0		0.0	−1	0.1247
4	−1	0.1464	−1	0.2150	−1	0.1350	−1	0.2052
5	+1	0.0373	+1	0.0240	+1	0.0048	−1	0.0300
6	−1	0.0063	−1	0.0391	−1	0.0126	+1	0.0156
7	+1	0.0448	+1	0.0283	+1	0.0070		0.0
8	−1	0.0236	−1	0.0303	−1	0.0441	−1	0.1548

Discussion

Structural models

An indication of the structure of the reaction center protein was obtained from model-building calculations, based on the scaled membrane profiles of Fig. 10 and information on the chemical composition of the reconstituted membrane. As a simple first approximation, the scaled model lipid profile of Fig. 11A (which is the step-function equivalent to Fig. 8) was subtracted from the scaled step-function equivalent membrane profile for the lipid to protein ratio of 150:1. The resulting difference profile due to reaction center protein was plotted either on a graph of electron density as a function of position along the membrane profile axis Z (where the protein is assumed to have a constant area throughout the profile) or on a graph of area as a function of Z (where the electron density of the protein was assumed to be constant throughout the profile (see Fig. 11)). Water content was included in all the protein profile calculations.

Linear combinations of the lipid model profile in Fig. 11A and the protein profile were then used to predict the membrane profiles for the lipid/protein ratios of 150, 100, 75 and 50: the calculated membrane model profiles are presented as step-function equivalent profiles $\rho_m(Z)$ in Fig. 12. These model step-function profiles were used to predict the integrated lamellar reflections (I'_m (h/D)) for each lipid/protein ratio (Fig. 12). The success of the prediction is reflected in the least-squares R value comparing I'_m (h/d) with the observed I' (h/D). The R values are given in Fig. 12 as R_I, which is the least-squares fit over the first four orders, and R'_I is the fit over the orders four through eight. The re-calculated integrated reflections I'_m (H/D) for the lipid/protein ratio of 150 should theoretically reproduce the observed integrated lamellar reflections; therefore, the R values for the I'_m (H/D) at this lipid/protein ratio reflect the inherent experimental errors, and hence approximately establish the accuracy expected of the model calculations at the other lipid/protein ratios. The R_I and R'_I values of the predicted lipid/protein model profiles for 100, 75 and 50 (Fig. 12B—D) molar ratios are large compared to the R fit for the profile of

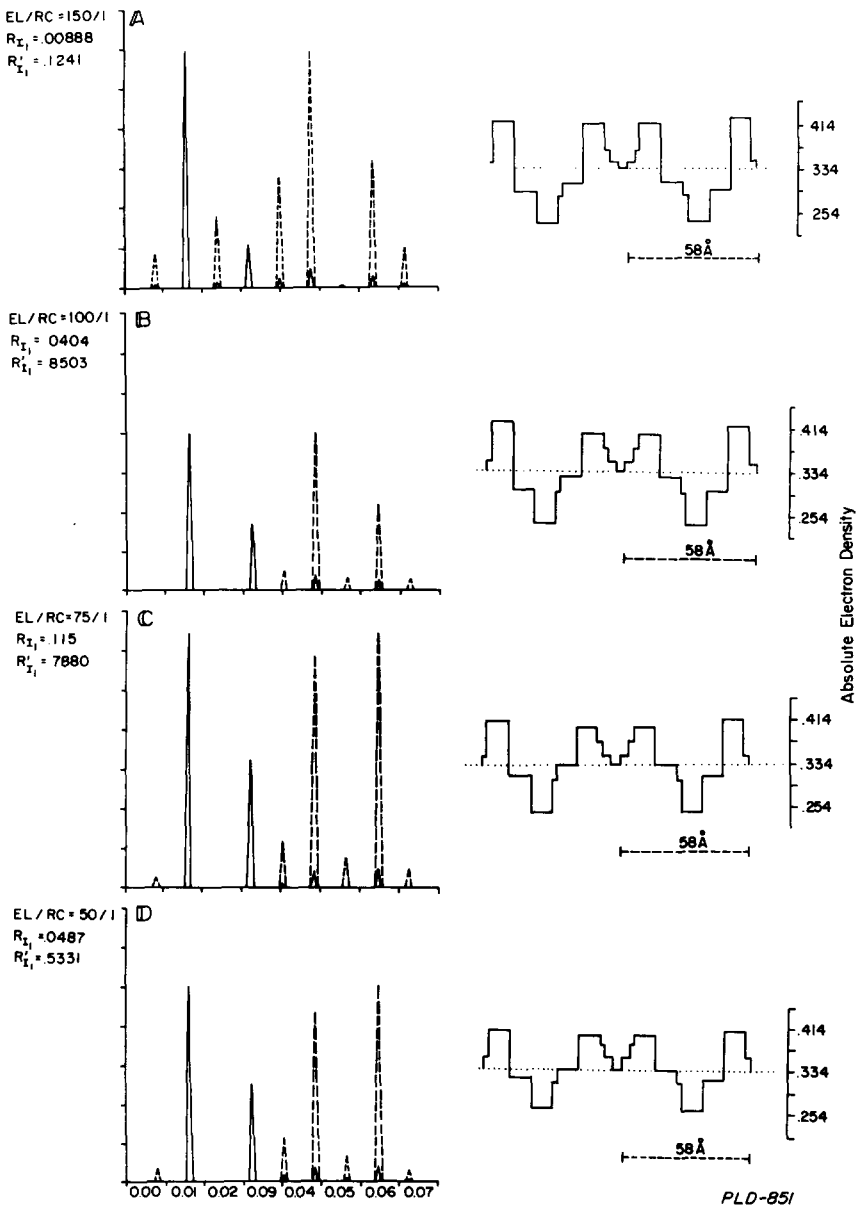

Fig. 12. Predicted lamellar reflections (left) and model membrane profiles (right) as derived from the protein and lipid profiles of Fig. 11. The R values for the predicted intensities are given for each lipid/protein ratio as R_I, which is the least-squares fit over the first four orders, and R_I' over the orders four through eight. The weaker intensities have been amplified (· · · · · ·). It can be seen from the R values that the lipid and protein models of Fig. 11 did not produce good predictions.

150 molar ratio (Fig. 12A). Also, a comparison of the model profiles for 100, 75 and 50 molar ratios of Fig. 12 with the corresponding step-function profiles of Fig. 10 reveals that the relative amplitudes of regions at the two membrane edges and the central region of the model profiles are not in good agreement

with the experimental profiles. If the model lipid profile of Fig. 11A was subtracted from the lipid/protein profiles of Fig. 10B, C or D, the resulting protein profiles were equally as ineffective in predicting the other three lipid/protein profiles via the model-building calculations.

Note also that the protein electron density profile in Fig. 11B has a relatively low region of electron density at 4 Å $< |z| <$ 14 Å. A larger electron density is expected in the regions close to the edge of membranes, as the hydrophilic amino acids have electron density greater than 0.4 $e/Å^3$ [29]; it is unlikely that this region would have an electron density of approximately 0.35 $e/Å^3$. Also, the average electron density for the calculated protein profile of Fig. 11B is 0.376 $e/Å^3$, significantly lower than the expected value of 0.410 $e/Å^3$, as calculated according to the method of Blaurock [29]. The inaccuracy of the protein profile, and consequently the predictions of the integrated lamellar reflections for the various membrane model profiles could possibly be attributed to a poor choice for the lipid model. It was therefore assumed, as a second approximation that the lipid polar headgroups may delocalize along the profile axis due to the presence of reaction center protein, and that such lipid delocalization could be asymmetric in the profile. Allowing for such delocalization, the widths of the lipid step-function equivalent model profile were changed to correspond to the widths of similar electron density regions in the experimental lipid/protein membrane profiles of Fig. 10; the regions were changed in such a way that the total area of the electron density profile was the same as Fig. 11A. This implicitly assumed that the lipid content on both sides of the membrane was equal. The modified asymmetric lipid model electron density profile allowing for lipid delocalization along the profile axis is pictured in Fig. 13A; the regions of 4 Å $< |z| <$ 16 Å and 16 Å $< |z| <$ 28 Å were changed from the analogous regions of Fig. 11A. This scaled lipid model profile was then subtracted from the scaled experimental lipid/protein membrane profile for a lipid/protein ratio of 100 in the way described above to produce the protein profiles of Fig. 13B and C.

As shown in Fig. 14, the resulting R_I and R_I' values reflect a substantial improvement over the model membrane profiles of Fig. 12. For instance, the low-angle R_I value was decreased by a factor of 23 for phosphatidylcholine/reaction center = 75/1, and by a factor of 10 for phosphatidylcholine/reaction center = 50/1. The third predicted lipid/protein model profile from this calculation (phosphatidylcholine/reaction center = 150/1) produced R_I = 0.0401 and R_I' = 0.1543 (not shown). However, if the protein profile of Fig. 13 was combined with the unaltered lipid profile of Fig. 11A, then R_I = 0.0044 and R_I' = 0.1208, which places the phosphatidylcholine/reaction center = 150 predicted profile within the same range of accuracy as the model membrane profiles of Fig. 14. Hence, it appears that one reaction center profile (Fig. 13) and two lipid profiles (Figs. 11A and 13A) are sufficient to explain our diffraction data suggesting that increasing the protein content of the membrane induces the delocalization of lipid polar head groups asymmetrically in the membrane profile.

The above result was obtained under the assumption that there is a strong lipid-protein interaction between phosphatidylcholine and reaction centers and that the lipid-protein forces dominate over lipid-lipid interactions; hence, as the protein content increased, lipid delocalization in the membrane profile would

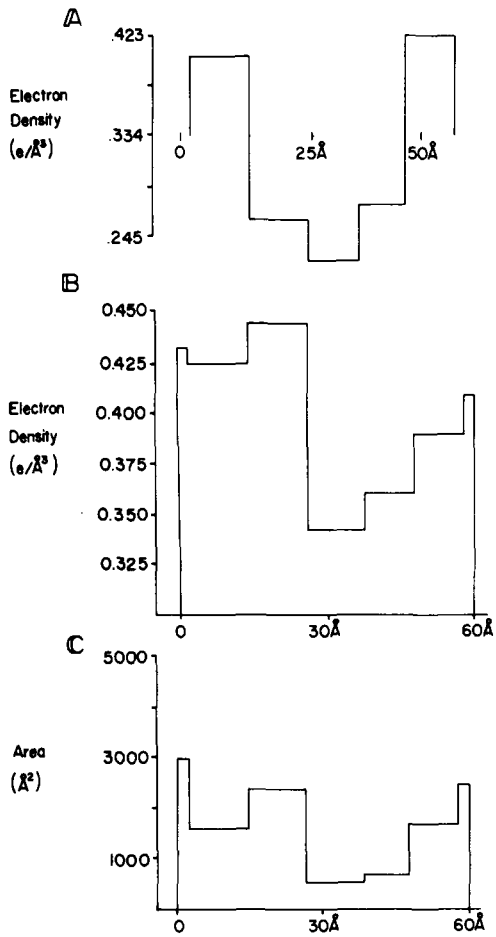

Fig. 13. (A) Second approximation of a model lipid profile, calculated by changing Fig. 11A slightly, assuming delocalization of the lipid polar head groups in the membrane profile more so on one side than the other. This model profile calculation also assumes that the total volume of lipid is not different on either side of the membrane from that of Fig. 11A. (B) Derived protein density profile, calculated by assuming a protein of constant area (as in Fig. 11B, except that the membrane profile of Fig. 10B was used, lipid/protein = 100). (C) Area profile for the protein calculated as in Fig. 11C.

be expected to increase. Conversely, under the less reasonable assumption that the reaction center protein profile be required to change in order to produce a reasonable prediction of the phosphatidylcholine/reaction center = 150 profile using the asymmetric lipid profile, then the protein density in the region of 4 Å $< |z| <$ 28 Å for the protein profile would have to increase significantly. The kinetic experiments similar to those reported in Figs. 2 and 3 support the premise that one protein profile should be employed to form the predicted lipid/protein model membrane profiles; the kinetic experiments revealed that the uniquely sided reaction of $(BChl)_2$ reduction by cytochrome *c* was not affected by changing the lipid/protein molar ratios, varying from 50 to 200.

Further investigations of the protein and lipid profile structures in these reconstituted membranes via neutron diffraction studies are in progress.

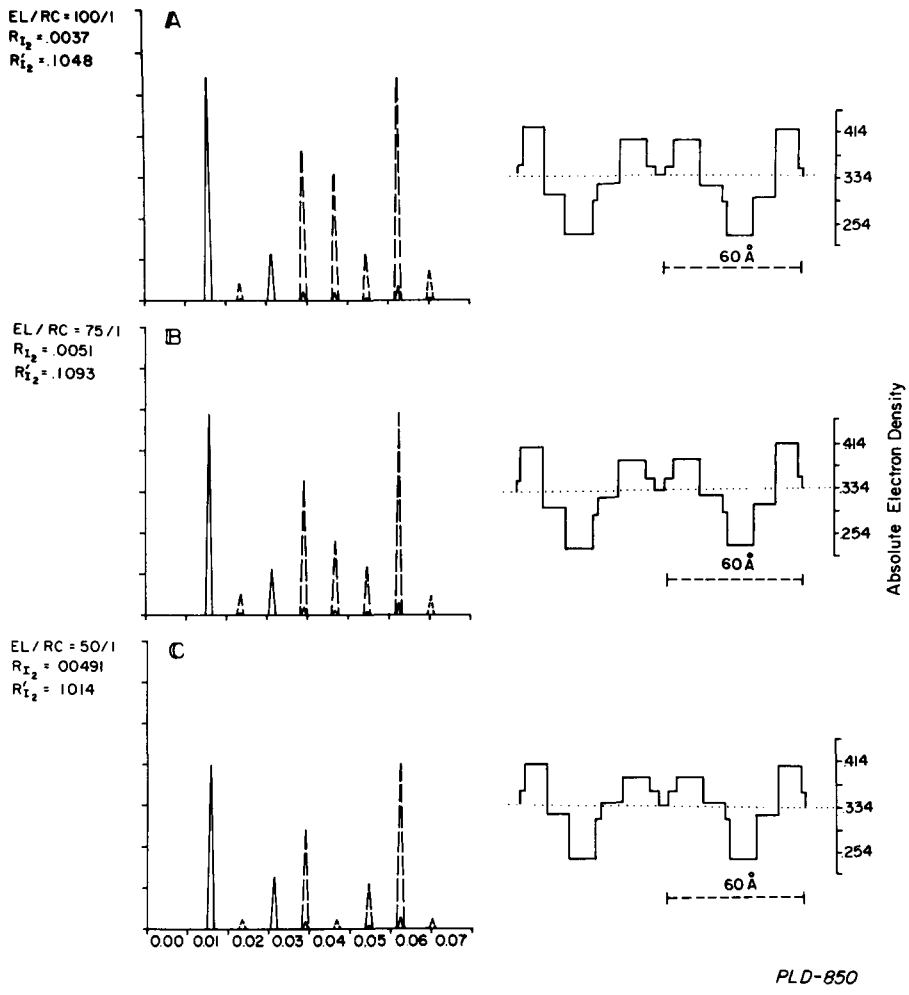

Fig. 14. Predicted lamellar reflections (left) and model membrane profiles (right) as derived from the protein and lipid profiles as in Fig. 13. Note that the *R* values have significantly improved over those of Fig. 12; the lipid and protein models of Fig. 13 yield good predictions.

Reaction center structure and orientation

In view of the good agreement between the model and experimental profiles obtained for membranes of various lipid/protein ratios (and hence agreement between the predicted and experimental integrated lamellar reflections), we feel that the lipid profiles of Figs. 11A and 13A, and the reaction center protein profile of Fig. 13 are reasonable approximations to their actual profiles.

The area plot of the reaction center protein profile in Fig. 13C was generated from the model calculations by assuming that the protein had constant electron density throughout the membrane profile. As can be seen, the protein would appear to have a gross shape similar to a 'dumbbell' with the area at either end of the protein near the membrane surfaces being about a factor of three larger than that near the center of the membrane. However, it may be difficult to

conceive of configurations of the phosphatidylcholine fatty acid chains that could conform to such large variations in the shape of the protein as shown in Fig. 13C. On the other hand, the electron density profile derived for the reaction center profile (Fig. 13B, which assumed that the protein has a constant area throughout the membrane profile) is another representation of the protein profile structure but it too suffers from inconsistencies. First, the average electron density of the calculated protein profile 0.395 $e/Å^3$ was slightly lower than the expected average electron density of 0.41 $e/Å^3$ [29]. Second, the amino acid composition of the three reaction center subunits suggest that large portions of the protein electron density profile cannot have electron density less than 0.38 $e/Å^3$ [29]; therefore, the region of 28 Å $< |z| <$ 48 Å in Fig. 13B would seem to have unaccountably low electron density. The true profile structure of the reaction center protein is probably a combination of Fig. 13B (varying electron density, with constant area) and Fig. 13C (varying area in the membrane plane, with constant electron density). However, these model calculations clearly indicate that the reaction center protein has a length of 60 Å in the membrane profile, that its spans the membrane profile and that its profile structure is rather asymmetric, there being more protein near one surface of the membrane than the other surface.

Finally, preliminary results from linear dichroism experiments verified that the orientations of the reaction center chromophores with respect to the membrane plane as measured in the reconstituted membrane system (in preparation) are similar to the reaction center chromophore orientations in *Rps. sphaeroides* R26 chromatophore membranes [30]. This result suggests that the orientation of the reaction center protein in the reconstituted membrane system is similar to the reaction center orientation in the chromatophore membrane.

Acknowledgments

We would like to acknowledge the contributions of Iris Torriani in the preliminary studies (Ref. 13). We are also indebted to Heather Bonner and Susan Samuels for their technical assistance and to Peggi Mosley for preparing the manuscript. The work was supported by a grant from the United States Public Health Service, GM 12202, and J.M.P. acknowledges his support from the Biomedical Research Support Grant, RR05415-16.

References

1 Okamura, M.Y., Steiner, L.A. and Feher, G. (1974) Biochemistry 13, 1394—1402
2 Feher, G. and Okamura, M.Y. (1977) Brookhaven Symp. Biol. 28, 183—193
3 Kaufmann, K.J., Dutton, P.L., Netzel, T.L., Leigh, J.S. and Rentzepis, P.M. (1975) Science 188, 1301—1304
4 Rockley, M.G., Windsor, M.W., Cogdell, R.J. and Parson, W.W. (1975) Proc. Natl. Acad. Sci. U.S. 72, 2251—2255
5 Dutton, P.L., Petty, K.M., Bonner, H.S. and Morse, S.D. (1975) Biochim. Biophys. Acta 387, 536—556
6 Prince, R.C., Baccarini-Melandri, A., Hauska, G.A., Melandri, B.A. and Crofts, A.R. (1975) Biochim. Biophys. Acta 387, 212—227
7 Dutton, P.L., Prince, R.C., Tiede, D.M., Petty, K.M., Kaufmann, K.J., Netzel, T.L. and Rentzepis, P.M. (1977) Brookhaven Symp. Biol. 28, 213—237
8 Blasie, J.K., Erecinska, M., Samuels, S. and Leigh, J.S. (1977) Biochim. Biophys. Acta 501, 33—52

9 Herbette, L., Marquardt, J., Scarpa, A. and Blasie, J.K. (1977) Biophys. J. 20, 245—272
10 Henderson, R. (1975) J. Mol. Biol. 93, 123—143
11 Santillan, G.G. (1976) Ph.D. Thesis, University of Pennsylvania
12 Pachence, J.M., Moser, C.C., Blasie, J.K. and Dutton, P.L. (1979) Biophys. J. 22, 55a (Abstr.)
13 Blasie, J.K., Torriani, I. and Dutton, P.L. (1974) Biophys. J. 14, 161a (Abstr.)
14 Pachence, J.M., Dutton, P.L. and Blasie, J.K. (1978) Biophys. J. 18, 9a (Abstr.)
15 Clayton, R.K. and Wang, R.T. (1971) Methods Enzymol. 23, 696—704
16 Clayton, R.K. and Haselkorn, R. (1972) J. Mol. Biol. 68, 97—105
17 Penna, F.J., Reed, D.W. and Ke, B. (1974) Proc. Int. Congr. Photosynth. Res. (Avron, M., ed.), Rehovot, Vol. 1, pp. 421—425
18 Parson, W.W. and Cogdell, R.J. (1975) Biochim. Biophys. Acta 416, 105—149
19 Singleton, W.S., Gray, M.S., Brown, M.L. and White, J.L. (1965) J. Am. Oil. Chem. Soc. 42, 53—63
20 Colowick, S.P. and Kaplan, N.O. (1957) Methods Enzymol. 3, 299—396
21 Dutton, P.L. and Wilson, D.F. (1974) Biochim. Biophys. Acta 346, 165—212
22 Kaufmann, K.J., Petty, K.M., Dutton, P.L. and Rentzepis, P.M. (1976) Biochem. Biophys. Res. Commun. 70, 839—845
23 Levine, Y.K. and Wilkins, M.H.F. (1971) Nat. New Biol. 230, 69—72
24 Stamatoff, J.B. and Krimm, S. (1973) Biophys. J. 16, 503—516
25 Schwartz, S., Gain, J.F., Dratz, E.A. and Blasie, J.K. (1975) Biophys. J. 15, 1201—1233
26 Klein, R.A. (1970) Biochim. Biophys. Acta 210, 486—489
27 Guinier, A. (1963) X-Ray Diffraction, W.H. Freeman and Company, San Francisco, CA
28 Schwartz, S. (1975) Ph.D. Thesis, University of California, Santa Cruz
29 Blaurock, A.E. (1972) Adv. Exp. Med. Biol. 24, 53—63
30 Vermeglio, A. and Clayton, R.K. (1976) Biochim. Biophys. Acta 449, 500—515
31 Demel, R.A., Geurts Van Kessel, W.S.M. and Van Deenen, L.L.M. (1972) Biochim. Biophys. Acta 266, 26—40
32 Overfield, R. and Wraight, C.A. (1978) Biophys. J. 18, 9a (Abstr.)